Published in final edited form as:
Neuroscience. 2011 July 14; 186: 188–200. doi:10.1016/j.neuroscience.2011.04.036.

Vagal intramuscular array afferents form complexes with interstitial cells of Cajal in gastrointestinal smooth muscle: Analogues of muscle spindle organs?

Terry L. Powley and **Robert J. Phillips**
Purdue University

Abstract

Intramuscular arrays (IMAs), vagal mechanoreceptors that innervate gastrointestinal smooth muscle, have not been completely described structurally or functionally. To delineate more fully the architecture of IMAs and to consider the structure-function implications of the observations, the present experiment examined the organization of the IMA terminal arbors and the accessory tissue elements of those arbors. IMA terminal fields, labeled by injection of biotinylated dextran into the nodose ganglia, were examined in whole mounts of rat gastric smooth muscle double-labeled with immunohistochemistry for interstitial cells of Cajal (ICCs; c-Kit) and/or inputs of different neuronal efferent transmitter (markers: TH, VChAT, and NOS) or afferent neuropeptidergic (CGRP) phenotypes. IMAs make extensive varicose and lamellar contacts with ICCs. In addition, axons of the multiple efferent and afferent phenotypes examined converge and articulate with IMA terminal arbors innervating ICCs. This architecture is consistent with the hypothesis that IMAs, or the multiply innervated IMA-ICC complexes they form, can function as stretch receptors. The tissue organization is also consonant with the proposal that those units can operate as functional analogues of muscle spindle organs. For electrophysiological assessments of IMA functions, experiments will need protocols that preserve both the complex architecture and the dynamic operations of IMA-ICC complexes.

Keywords

mechanosensitive afferents; mechanoreceptors; smooth muscle; stomach; stretch receptors; vagus nerve

Section 1.1

The vagus nerve supplies two morphological distinct mechanoreceptors to the smooth muscle layers of the gastrointestinal tract. Of these two kinds of mechanoreceptors, *intraganglionic laminar endings* (IGLEs) were the earlier to be identified, and they have been characterized both structurally (e.g., Lawrentjew, 1929; Rodrigo et al., 1975; Raab and Neuhuber, 2004) and functionally (Zagorodnyuk et al., 2001; Brookes et al., 2005). In

Corresponding author: T.L. Powley Purdue University, 703 3rd Street, West Lafayette, IN 47906, powleytl@psych.purdue.edu, Phone: 765-494-6269, Fax: 765-496-1264.

Competing Interests: the authors have no competing interests.

contrast, *intramuscular arrays* (IMAs), the more recently described of the vagal afferent mechanoreceptors to gut smooth muscle, have been less fully described structurally, and their functions have not been adequately characterized.

The facts that IMAs form terminal arrays of parallel telodendria coursing within the muscle wall and parallel to smooth muscle fibers (Berthoud and Powley, 1992), contact interstitial cells of Cajal of the intramuscular type (ICC1; Powley et al., 2008), and are concentrated in particular regions, notably the forestomach and major sphincters (Wang and Powley, 2000), lead us to hypothesize that IMAs may operate as stretch detectors that report stretch or length of muscle in the gut wall (Phillips and Powley, 2000; Powley and Phillips, 2002).

Electrophysiological analyses of vagal afferents, however, have not provided an unambiguous assessment of the function(s) of the IMAs. Most of the electrophysiology on vagal afferents to the GI tract was performed before IMAs were identified. Because of this chronology, neither the gut regions sampled nor the mechanical and chemical stimuli administered in earlier experiments allow unequivocal re-mapping or re-interpretations of the observations in terms of the later information on the structure or the distributions of IMAs. A few neurophysiological analyses of gut afferents are more recent, but the function(s) of IMAs still remain enigmatic. In the most extensive of the recent electrophysiological surveys, Brookes and Zagorodnyuk, and their coworkers, exposed samples of gut wall *in vitro* to controlled manipulations of tension, mapped single unit receptive fields within the specimens, and then stained the visceral terminals in the preparations by applying a tracer to nerve bundles entering the specimen. The Brookes-Zagorodnyuk protocol elegantly characterized a tension receptor function for IGLEs (Zagorodnyuk et al., 2001). Importantly, though, the investigators also discovered that the particular tissue preparation, recording bath, and stimulus conditions that effectively profiled IGLEs did not successfully activate the IMAs that were labeled with tracer and mapped in the experiment (also see discussion in Brookes et al., 2005). To the best of our knowledge (see also Zagorodnyuk et al., 2010), the experimental conditions needed for activating and electrophysiologically characterizing IMAs have yet to be delineated.

Given the limited structural information available on IMAs and given the ambiguities associated with structure-function correlations for IMAs, the present experiments were designed to provide additional anatomical information about the organization of these afferents. Previously, extensive morphological characterizations proved crucial for the functional analyses of cutaneous and proprioceptive mechanoreceptors (e.g., Andres and Düring, 1973; Iggo, 1976; also cf. Zagorodnyuk et al., 2010) as well as, of course, IGLEs (e.g., Lawrentjew, 1929; Rodrigo et al., 1975; Zagorodnyuk et al., 2001; Raab and Neuhuber, 2004; Brookes et al, 2005) , and, arguably, they will be equally critical in the case of IMAs. Thus, we have performed a series of double labeling experiments that seemed particularly relevant in light of ultrastructural evidence that IMAs, as they arborize and innervate ICCs, are found in small bundles of axons of unknown origins and phenotypes (Powley et al., 2008; also see Huizinga et al., 2008). Presumably, and as also argued by others (e.g., Zagorodnyuk et al., 2010), such a fuller understanding of the structural organization of the vagal mechanoreceptor endings is needed and may provide observations that will help in the development of future neurophysiological and functional assessments of the afferent enigmas called IMAs.

[1]Spindle-shaped intramuscular Interstitial cells of Cajal in the smooth muscle layers are commonly distinguished from other types of ICCs with the designation of “ICC-IMs.” For brevity and simplicity, however, since all references to interstitial cells of Cajal throughout the present report refer to this intramuscular type, the generic designation “ICC” is used.

2.1 EXPERIMENTAL PROCEDURES

2.1.1 Subjects

Virgin male Sprague-Dawley rats (n=40) were purchased from Harlan (Indianapolis, IN, USA) at 3 months of age, and housed in an AAALAC-approved colony room on a 12 h light/dark schedule with chow (laboratory diet No. 5001; PMI Feeds, Inc., Brentwood, MO, USA) and water available *ad libitum*. Every effort was made to minimize suffering and the number of rats used, and all procedures were conducted in accordance with the National Institutes of Health *Guide for the Care and Use of Laboratory Animals* (NIH Publications No. 80-23) revised 1996, and approved by the Purdue University Animal Care and Use Committee.

2.1.2 Selective labeling of the vagal afferent innervation of the stomach

The neural tracer Mini-Ruby (dextran, tetramethylrhodamine and biotin; 10,000 MW, lysine fixable; D3312; Invitrogen, Carlsbad, CA, USA) injected into the nodose ganglia labels selectively vagal sensory axons and terminals innervating the smooth muscle wall of the gastrointestinal tract (Powley and Phillips, 2005). Tracer injection surgery consisted of overnight food-deprived rats being anesthetized with sodium pentobarbital (60 mg/kg, i.p.), and then having their left and right nodose ganglia exposed by blunt dissection and a solution of 10–15% Mini-Ruby pressure injected through a glass micropipette (ID 25 μm) into each ganglion (2–3 μl/ganglion). The skin was then closed with interrupted sutures and treated with antibacterial powder, and the rats were allowed to recover on a warming pad before being returned to their home cages.

Fifteen days post-injection, rats were killed with a lethal dose of sodium pentobarbital (180 mg/kg, i.p.) and transcardially perfused with physiological saline followed by 4% paraformaldehyde in 0.1 M PBS (pH 7.4). The stomachs were removed and divided into dorsal and ventral whole mounts by cutting along the greater and lesser curvatures, and then rinsed and fixed an additional 12–24 h in the same fixative. The mucosa and submucosa were then removed by fine dissection, resulting in stomach whole mounts consisting of the smooth muscle layers. Free-floating whole mounts were then rinsed in PBS, incubated for 30 min in a hydrogen peroxide:methanol (1:4) block to quench endogenous peroxidase, rinsed in PBS, and soaked for 3–5 d at room temperature in a PBST block (PBS containing 0.5% Triton X-100 and 0.08% Na Azide). Whole mounts were then rinsed in PBS, incubated for 1 h in avidin-biotin-horseradish peroxidase complex (PK-6100; Vectastain Elite ABC Kit, Standard; Vector Laboratories, Inc., Burlingame, CA, USA), rinsed in PBS, and reacted with diaminobenzidine (DAB) and H_2O_2 for 5 min to yield a permanent golden-brown deposit. Finally, stained whole mounts were rinsed in distilled water, mounted on gelatin-coated slides, air-dried overnight, dehydrated in alcohol, cleared in xylene, and coverslipped with Cytoseal (Richard-Allan Scientific, Kalamazoo, MI, USA).

2.1.3 Immunohistochemistry

Permanent labeling of the Mini-Ruby filled vagal sensory terminals was combined with immunohistochemstry to study the relationship of the endings to other neural structures located in the smooth muscle wall of the stomach. All of the immunohistological procedures were done at room temperature. Following endogenous peroxidase block, stomach whole mounts from rats injected bilaterally into the nodose ganglia with Mini-Ruby were soaked for 3–5 d in PBST with the addition of the appropriate normal serum (donkey or horse) followed by overnight incubation with a primary antisera in the same diluent. Details of the primary and secondary antisera used are listed in Table 1. No immunoreactive structures were detected when the primary antiserum was omitted. After incubation with a primary, whole mounts were then soaked in ABC solution followed by staining of the Mini-Ruby

filled terminals with DAB. Whole mounts were then rinsed with distilled water, washed again with PBST, exposed for 2 h to the relevant secondary antiserum, rinsed in PBS, incubated 1 h in ABC, rinsed with PBS, and then reacted for 3 min with Vector VIP (SK-4600; Vector Laboratories, Inc.) substrate which resulted in an intense, violet-colored precipitate that contrasted nicely with the DAB. Whole mounts were then rinsed in distilled water, mounted on gelatin-coated slides, air-dried overnight, dehydrated in alcohol, cleared in xylene, and coverslipped with Cytoseal.

Initial screening of the stomach whole mounts revealed that vagal sensory terminals located in the smooth muscle are in close registration with c-Kit-positive interstitial cells of Cajal (ICC) and TH+ and CGRP+ fibers, so additional stomach whole mounts from unoperated controls were double labeled for c-Kit and either TH or CGRP to determine if TH+ and CGRP+ also contact ICCs. In addition, stomach whole mounts from unoperated control rats were double labeled for c-Kit and either NOS or VChAT to illustrate the well documented innervation of ICCs by both inhibitory and excitatory enteric motor neurons (Burns et al., 1996; Ward et al., 2000; Ward and Sanders, 2001). Briefly, whole mounts from control rats transcardially perfused with physiological saline followed by 4% paraformaldehyde were blocked for endogenous peroxidase, soaked for 5 d in the appropriate normal serum block, and then incubated overnight in a cocktail of primaries which always consisted of c-Kit and either TH, CGRP, NOS, or VChAT. Whole mounts were then rinsed with PBST, soaked for 2 h in the appropriate anti-mouse or anti-goat secondary, followed by 1 h in ABC and then reacted for 5 min in DAB. Whole mounts were then rinsed in PBS, rinsed again in PBST, soaked for 2 h in the appropriate anti-goat secondary, followed by 1 h in ABC and 3 min in Vector VIP to visualize the ICCs . Finally, stomach whole mounts were mounted on slides, air-dried overnight, dehydrated in alcohol, cleared in xylene and coverslipped with Cytoseal.

2.1.4 Photography and image post-processing

Images were acquired using a LEICA DM microscope and either a SPOT RT KE camera or a SPOT Flex camera, both controlled using SPOT Software (V4.7 Advanced Plus; Diagnostic Instruments, Sterling Heights, MI). Final figure production was done using both the SPOT software and Photoshop CS4 (Adobe Systems, San Jose, CA). To maximize the depth of field of images taken from the thick stomach whole mounts, Helicon Focus Pro X64 (Version 5.1.23; HeliconSoft Ltd., Kharkov, Ukraine) was used to merge a series of shots that were taken at different focal distances into a single image with enhanced depth of field (i.e., focus stacking; Gulbins and Gulbins, 2009). Photoshop CS4 was used to: (1) apply text and scale bars; (2) adjust color, brightness, contrast, and sharpness; (3) remove artifact (done sparingly and explicitly stated in the appropriate figure legend when applied); and (4) organize the final layout of the figures. Additionally, Photoshop CS4 was used to adjust hue to provide the best contrast between the DAB (brown) and Vector VIP (violet) labeled fibers. Finally, the Neurolucida software package (MicroBrightField, Inc., Williston, VT, USA) was used to trace and illustrate the morphology of individual terminals.

3.1. RESULTS

3.1.1 IMA-ICC Organization

IMA afferents coursed within distal vagal branches and myenteric connectives distributing through the gut wall and then projected into a muscle layer where they arborized into terminal arrays of parallel telodendria (e.g., Figure 1). These neurites coursed in conjunction with the interstitial cells of Cajal running parallel to the bundles of smooth muscle fibers (e.g., Figures 2 and 3), as has been previously described. In addition, though, the present series of tissue specimens in which IMAs were labeled with dextran and ICCs were stained

by immunohistochemistry for c-Kit, highlighted several additional features of these IMA-ICC complexes.

Notably, the primary neurites of IMA afferents separated from vagal bundles or myenteric connectives and then travelled in smaller bundles and then finer fascicles, to traverse their respective muscle sheets and reach their terminal fields. Though it has been shown that IMA fibers travel through the muscle wall in small nerve fascicles (see Powley et al., 2008), the present labeling of vagal afferents suggests that these fascicles contain a single — or a few--IMA fibers, with the other neurites being non-vagal (see below). Between the point of separation from the larger afferent fiber bundles and the terminal arbors of the individual afferents, the IMA afferent fibers tended to travel obliquely to the vector or primary orientation of the muscle fibers within the sheet. As fibers approached their respective terminal fields, they bifurcated repeatedly to produce their terminal arrays (Figure 1). The parallel and rectilinear organization of the IMA afferent terminal arrays corresponded very closely with or appeared dictated by the local organization of the ICCs which were distributed in strings or chains running parallel to the neighboring bundles of smooth muscle fibers (Figure 2). Specifically, the IMA afferent terminals repeatedly bifurcated and generated short bridging elements as needed so that long processes of the terminals then ran along — and in contact with — strings or courses of the ICCs. With this architecture, the IMA terminal arrays also paralleled the primary axis of the smooth muscle fibers.

Proximal to their terminal arbors, IMA afferent neurites tended to be relatively smooth, issuing only a few short spurs (Figure 1C). As the fibers reached the networks of ICCs they innervated, they then often elaborated numerous leafy varicosities or lamellar plates, some of them having resemblances to filopodia (see Figures 1, 2, 3A, 3B and 3C). Notably, too, in their terminal fields IMA neurites in some instances issued short spurs and collaterals that extended away from the ICC scaffolds, into bundles of muscle fibers, and then appeared to divide or branch so as to produce short arms that ran within the bundles and parallel to the muscle fibers (Figures 2A and 2B). Though lamellar IMA varicosities were concentrated where the afferents ran in close association with ICCs, they also occurred in the short side arms and in the short bridging elements that interconnected the longer neurites running with ICCs (Figure 2B; also Figure 3B).

Assuming that an IMA terminal — or the complex that its arbor forms with ICCs — comprises the receptive field of that afferent, another feature of the IMA innervation of ICCs may have functional significance: IMA neurites ramified in patterns that distributed the linear terminals of the array over a limited number of adjacent strings of ICCs, strings typically in one bundle — or a few neighboring bundles--of muscle fibers defined by major connective tissue septa. Furthermore, any single string of ICCs seemed to be contacted by a neurite or neurites of only one IMA terminal array. [It needs to be stressed that the tracer injections used did not label all vagal afferents in any given animal, but still, in a substantial sample of specimens, we did not observe terminal neurites of two or more independent IMA afferents converging on the same chain of ICCs.]

IMA terminal arbors varied in length, and their neurites varied in number and degree of varicosity. In terms of overall length, IMAs varied from region to region. Circular muscle IMAs in the corpus, for example, spanned considerable distances (cf. Fig. 1), whereas IMAs in the sphincters tended to be substantially shorter. Furthermore, the number of individual IMA neurites forming a given array varied by location (e.g., corpus circular muscle IMAs typically consisted of several neurites whereas circular muscle IMAs found in and near the pylorus were comprised of many more individual processes). IMA terminal neurites often elaborated conspicuous lamellar varicosities (see Figure 3A, 3B and 3C), but the pattern was not invariant. Some IMA neurites —or segments of neurites— displayed only modest

swellings or dilations without substantial lamellar varicosities (Figure 3D and 3E). Notably, even within the same IMA the neurites varied in the complexity and number of varicosities (e.g., Figure 1B or 1D).

3.1.2 IMA and CGRP+ fiber Distributions

Since small bundles of heterogeneous axons run in proximity to ICCs (e.g., Gabella, 1989; Mitsui and Komuro, 2002; Huizinga et al., 2008) and since we observed--in a recent ultrastructural study that included tracer-labeled IMAs--these bundles frequently contain only one or two IMA fibers and several axons unlabeled with dextran (Powley et al., 2008; also see Figures 4A and 5A), we evaluated a series of specimens in which IMAs were labeled with dextran, or ICCs were processed for c-Kit, and immunohistochemistry was used to identify CGRP+ neurites.

CGRP-positive fibers could regularly be observed running tightly in tandem with the terminal arbors of IMA neurites. These associations occurred both along the long straight IMA elements that are characteristically seen on ICCs (Figure 4B through E). In addition, when tissue double-labeled for CGRP and for c-KIT, varicose CGRP+ neurites were seen coursing on the network of ICCs (Figure 6G and 6H). CGRP+ neurites also were observed to continue along with the IMA bridging elements that ran from one string of ICCs to a neighboring string (Figure 4F). Notably, though, CGRP+ fibers, after coursing some distance in registration with the IMA afferent would often separate and run independently in smooth muscle, commonly but not exclusively parallel to the muscle fibers, for some distance. The CGRP+ fibers associated with the IMA terminal arbors were typically fine varicose neurites. At the point where the terminal arbors of IMA afferents were observed in contact with ICC chains, the CGRP-positive projections consisted of only one or two isolated fibers.

3.1.3 IMA and TH+ fiber Distributions

To evaluate whether presumptive extrinsic efferent fibers might also associate closely with the IMA-ICC complexes, distributions of tyrosine hydroxylase-positive or “TH+” fibers (as well as cholinergic and nitrergic —see below) were compared with c-Kit labeled ICCs and with dextran labeled IMAs in the stomach wall.

In specimens in which the double labeling consisted of dextran-labeled IMAs and TH+ axons, individual IMA neurites could be seen coursing in tandem with individual (one to two) varicose TH+ axons (Figure 5).

Networks of ICCs in the muscle sheets were extensively innervated by TH+ axons. As illustrated in Figure 6 (panels E and F), individual TH+ axons were found running parallel to the smooth muscle fibers. Some of the TH+ fibers appeared to run within bundles of muscle without any close associate to ICCs, but the of majority of TH+ fibers were observed to run in close proximity to the chains of ICCs found within the muscle bundles. The majority of strings of ICCs appeared to have one or two varicose TH+ fibers in close apposition.

3.1.4 ICCs and NOS+ and VChAT+ Fiber Distributions

Though our sample of specimens of these two phenotypes was more limited and our double labeling was confined to cases in which one of the two transmitter phenotypes was labeled in conjunction with c-Kit immunohistochemistry to label ICCs, the innervation patterns were similar to those of CGRP and TH (Figure 6C and 6D) . For both NOS+ fibers VChAT + fibers, the double-labeled specimens indicated that individual (one or two neurites) of the phenotype innervated and formed close appositions with the ICC chains in the smooth muscle wall.

4.1 DISCUSSION

The present double-labeling experiments revealed several previously unreported structural features of IMAs and their accessories tissues that have functional implications: The experiments demonstrate for the first time that axons of three different phenotypes of efferents (TH+, VChAT+, andNOS+) and one phenotype of afferent (CGRP+) intermingle with terminal neurites of IMAs as these vagal afferents form complexes with strings of ICCs. Additionally, IMAs produce extensive and numerous lamellar varicosities as they establish complexes with ICCs. Finally, IMAs extend spurs or short collaterals to insinuate between muscle fibers adjacent to the IMA-ICC complexes. These new observations can be discussed in terms of three sets of issues: 1.) A reconsideration of the conventional “free nerve ending” idea for vagal IMAs; (2) A consideration of the IMA-ICC complex as a smooth muscle functional analogue of the striated muscle spindle organ; (3) An assessment of implications of the present structural observations for attempts to study IMAs electrophysiologically.

4.1.1 Are IMAs “free nerve endings?”

Even though vagal afferents are not encapsulated and have traditionally been treated as free nerve endings, the present observations underscore the fact that IMAs are not conventional free nerve endings. This distinction has implications for receptor operations. In the instance of free nerve endings that are not associated with accessory tissue specializations, the afferent terminals themselves are presumed responsible for transducing stimuli. Such elements are often assumed to be broadly tuned and polymodal. In contrast, in the case of afferents that articulate with organized accessory tissue elements, the mechanical, biochemical and electrophysiological properties of surrounding tissues typically shape the transduction processes (Andres and D ring, 1973; Iggo, 1976; Liem and van Willigen, 1985). Two features of IMA terminal arbors are likely to be important in translating mechanical stimuli into afferent activity. The first feature is the elongated arrays of parallel afferent terminals, and the second is the specialized organization of the IMAs in close association with ICCs and other afferent and efferent axons.

As previously described and as illustrated in the present observations, IMAs are highly elongated, often extensive, parallel arrays of neurite terminals that run within the smooth muscle layers. In the case of cutaneous mechanoreceptors, such elongated terminals are known to have highly polarized or directional sensitivities and receptive fields (MacIver and Tanelian, 1993). Muscle spindle organs (see discussion below), of course, are also polarized and oriented to detect stretch or length along their long axes, which parallel the extrafusal muscle fibers. Such examples reinforce the hypothesis that IMAs are structured so as to be more sensitive to mechanical forces operating on the long axis and less sensitive to forces operating in an orthogonal direction.

IMAs establish extensive and close appositions with ICCs running parallel to muscle fibers. Previous observations have indicated that IMA varicosities contacting ICCs form synapse-like contacts (vesicles, prejunctional thickenings, etc.) with ICCs (Powley et al., 2008; see also Huizinga et al., 2008), and the present observations now illustrate how numerous such varicosities are (see, for example, Figures 1, 2 and 3). The extensive numbers of contact sites of IMAs with ICCs underscore the possibility that IMAs may carry stretch or length signals that originate or are transduced within the ICC-muscle-fiber apparatus of the gut (Huizinga et al., 2010). Both GI smooth muscle fibers (Won et al., 2005; Kraichely and Farrugia, 2007) and ICCs (Won et al., 2005; Kraichely and Farrugia, 2007) have been shown to transduce stretch or length signals. This information is integrated into the motor and pacemaker functions of the respective tissues (cf. Sanders et al., 2010; but also see Goyal and Chaudhury, 2010), but it may also provide, concomitantly, a transduction

mechanism for IMAs. In addition, smooth muscle (Kraichely and Farrugia, 2007; Sanders and Koh, 2007), ICCs (Kraichely and Farrugia, 2007), and vagal afferents (Bielefeldt et al., 2006; Smid, 2009; Brierley 2010) all have been shown to express mechanosensitive channels, consistent with the possibility that the different elements may work cooperatively or synergistically to transduce specific stretch or muscle length information.

4.1.2 IMA-ICC complexes may be functional analogues of muscle spindle organs

Additional features of the architecture of IMA-ICC complexes reinforce the suggestion that these complexes organize dynamic and integrated sensorimotor responses analogous to adjustments organized by striated muscle spindle organs.

First, as described in of the present observations, before reaching their target ICCs, IMAs course in close registration with a multiplicity of efferents and other afferents of different phenotypes known to influence ICC function. Specifically, the present double-labeling series illustrates, through the multiple pair-wise combinations, that individual IMA fibers and individual afferents and efferents of the different phenotypes intermingle extensively as they travel to their common ICC targets. The different elements tend to course together in close registration, making it plausible that the fibers are co-mingled in the same small fascicles of axons projecting to ICCs (Mitsui and Komuro, 2002; Huizinga et al., 2008; Powley et al., 2008). The multiplicity of varicosities interspersed along the fascicles would be consistent with interactions among the processes.

Second, the convergence of the three types of efferents (TH+, NOS+, and VAChT+ fibers; see Fig. 6) and the two types of afferents (namely the vagal IMAs and CGRP+ presumptive visceral afferents; see Figs. 2 and 6) on ICCs underscores the suggestion that IMA-ICC complexes are specialized “organs” reminiscent of striated muscle spindle organs. This heterogeneity of converging projections suggests that the IMAs or IMA-ICC units could be dynamically tuned and influenced by multiple feedback and feedforward loops. Consistent with the present observations and idea that IMA activity may reflect the complex integration occurring in the IMA-ICC complexes, ICC pacemaking and activity has previously been shown to be modulated by catecholaminergic (Jun et al., 2004), nitrergic (Zhang et al., 2010), and cholinergic (Ward et al., 2000; Zhang et al., 2010) signals. Furthermore, and correspondingly, in different immunohistochemical experiments, these axonal phenotypes have also been previously observed in close apposition to ICCs: TH+ axons (Cobine et al., 2009), NOS+ neurites (Salmhofer et al., 2001; Cobine et al., 2009), and VAChT+ processes (Ward et al., 2000; Beckett et al., 2003). The present observations replicate these earlier structural observations, but, more importantly, also establish that one and the same ICCs are innervated by IMAs and the different efferent inputs. In addition, the present series with immunohistochemistry for CGRP+ axons suggest that, in addition, IMA-ICC complexes are also innervated by at least a second type of visceral afferent.

Third, the prominent lamellar varicosities observed on many IMA terminal neurites and the varicosities of the CGRP+ fibers could reflect integrative sensorimotor functions over and above the fundamental sensory signaling roles of the afferents. Electrophysiological evidence (e.g., Wei et al., 1995) has suggested that vagal afferents may coordinate peripheral processing and integration with “axon responses” or “axon reflexes” that involve local peripheral release of neuromodulators. Even more particularly, there is both electrophysiological (Zagorodnyuk et al., 2001; Brookes et al., 2005) and morphological (Raab and Neuhuber, 2004; Powley et al., 2008) evidence that IGLEs may use axon responses for local signaling. Furthermore, another feature of the vagal afferent innervation of the GI smooth muscle wall is consistent with axon-response signaling: The initial description of IMAs (Berthoud and Powley, 1992) noted that a vagal afferent neurite can terminate with one collateral forming an IMA and another branch forming IGLEs and

suggested the possibility that such an organization might support axon reflex activity. Subsequent surveys (Wang and Powley, 2000; Powley and Phillips, 2002, 2005) have indicated that individual afferents commonly form either IMAs or IGLEs, not both, and only a small percentage of the vagal afferents to smooth muscle form polytopic hybrid endings, but, nonetheless, this limited population of complex afferents is situated in a manner that could generate axon reflexes which might integrate or cross-couple tension signals transduced by IGLEs and stretch signals transduced by IMA-ICC complexes. Additionally, also consistent with the axon response possibility, CGRP is implicated in axon responses in other visceral tissues (e.g. Gokin et al., 1996; Chang et al., 2000). More specifically then, in the case of IMAs, the possibility that afferent axon responses might play roles in the coordination and/or other operations of IMA-ICC complexes is suggested by (1) our earlier ultrastructural observation that IMA varicosities contain vesicles (Powley et al., 2008), (2) the present observations of extensive lamellar varicosities on IMA terminals innervating ICCs (e.g., Figures 1D, 3A, 3B, 3C), as well as (3) our new finding that varicose CGRP+ neurites intermingle with IMA terminal neurites complexing with ICCs (e.g., Figure 4F). As an alternative— but not a mutually exclusive alternative--to the axon response idea, the plate-like varicosities of IMAs might effectively serve a mechanical function such as tethering the IMAs or IMA-ICC complexes to surrounding tissue elements (also see below).

Finally, an additional feature also suggests that IMAs are situated to code— and potentially to reciprocally control —a variety of local muscle, as well as ICC, conditions. As noted in the present observations (e.g., Figure 2A and 2B), the spurs and short side arms that IMAs extend, without paired ICC elements, among muscle fibers, suggest that the vagal afferents may be influenced directly by muscle fiber conditions, as well as by ICC activity. More particularly, it is plausible that the IMA side arms insinuated between muscle fibers and the IMA varicosities attached to ICCs create anchor points so that the afferents undergo shearing and deformations when muscle length changes.

4.1.3 Assessing receptor functions of IMA-ICC complexes experimentally

As noted by Kraichely and Farrugia (2007; see also Brookes et al., 2005), it is difficult to reproduce, under *in vivo* conditions, the mechanical forces to which different mechanosensitive neurons are exposed under native circumstances. In all likelihood, the common difficulties in achieving those conditions for any mechanoreceptor are compounded (1) when the neuronal terminals are distributed over considerable distances, as are IMAs (making it more difficult to preserve the integrity of the endings during surgical exposure), (2) when the terminals are highly oriented, as are IMAs (making it difficult to align mechanical forces with an unstained fiber of an unspecified orientation under *in vivo* conditions), and (3) when the terminal arbors have non-uniform and limited regional distributions, as do those of the IMAs (Wang and Powley, 2000).

Given the hurdles to producing focal, limited, and precise manipulations of IMAs, *in situ*, under physiological conditions (cf. Brookes et al., 2005), non-specific stimulation becomes a problem. Since vagal afferents, ICCs, and gut smooth muscle all express mechanosensitive channels, even non-specific distortions or displacements of the tissues would be expected to elicit some neuronal activity, and it becomes important to assess whether any elicited activity reflects only non-specific responses that don't represent any of the transduction selectivity or sensory tuning that the afferents normally receive from their accessory tissues.

Furthermore, because of the geometry and biophysics of highly distensible hollow organs such as the gut, most manipulations of wall tension concomitantly produce changes in stretch, and most manipulations of stretch change tension. Much of the electrophysiology of gastrointestinal smooth muscle has not explicitly and/or experimentally distinguished "tension" and "stretch" and the two modalities have at times been discussed

interchangeably. The few electrophysiological experiments that have attempted to manipulate gut wall tension and stretch independently (e.g., Leek, 1969 Blackshaw et al., 1987) have recognized practical problems in achieving orthogonal manipulations. For example, in attempting to interpret their results, Blackshaw and colleagues (1987) stressed that their experiment had failed to achieve an effective isotonic condition and noted, presciently, that experimental uncertainties were created by the lack of a morphological description of the afferent receptors. Instructively nonetheless, even though their work pre-dated the discovery of IMAs and the investigators designed their experiment to investigate a single type of receptor, Blackshaw and colleagues (1987) observed two patterns of unit responses, concluded that gastric mechanoreceptors are not a homogenous population, and reported that afferent discharge rates of some neurons track changes in muscle length when tension does not change. Experimental challenges notwithstanding,an unambiguous assessment of the mechanosensitivities of IMAs (as well as IGLEs) will likely need to deliver stretch stimuli under isotonic conditions and tension stimuli under isometric conditions, with (1) the gut relatively intact, (2) the experimental stimuli administered in an orientation to engage putative stretch- or length- detection, and (3) the test stimuli directed to the appropriate gut regions where the endings are concentrated.

Other impediments to evaluating IMAs as part of an IMA-ICC stretch receptor complex may stem more from the interdependent organization of these complexes. If IMA operations depend on the state of the ICCs and the muscle fibers that the ICCs pace, then selective experimental activation of the IMA is likely to be practical only when a given protocol both preserves the entire afferent terminal and maintains the tone of the muscle as well as the associated ICCs. Like the relative unresponsiveness of annulospiral ending fibers innervating striated muscle spindles when extra- and intra-fusal muscle fibers have lost their tone or are operating outside of their dynamic ranges, IMAs may only be capable of representative, graded, and sensitive responses when the entire IMA-ICC unit and associated muscle fibers are working in their physiological ranges.

Paradoxically, it seems instructive that past electrophysiological surveys have had little success finding evidence of a vagal stretch receptor in the stomach wall. The absence of positive identifications of afferents with stretch receptor functions could signal a dearth of such afferents in the gut, but the same absence of identifications could, of course, equally readily signal only that most previous paradigms have been inefficient or inappropriate for capturing the physiology of IMAs. By extension, the lack of success in functionally characterizing IMAs could even be construed as indirect support for the conclusion that IMA function needs to be examined with recording protocols that preserve the integrity and dynamic operations of IMA-ICC complexes and that vary tension and stretch independently.

Acknowledgments

For their expert technical assistance, we thank Elizabeth Baronowsky (tracer injections) and Julia Pairitz (immunohistochemistry). In addition, we thank Cherie N. Billingsley and Jared Gilbert for their help in tracing and mapping IMA profiles. The project described was supported by Awards R37DK027627, R01DK61317, and P01 HD052112 from the National Institutes of Health. Both authors contributed to the design, data analysis, and write-up of the experiment.

References

Andres, KH.; Düring, MV. Morphology of cutaneous receptors. In: Iggo, A., editor. Handbook of Sensory Physiology. 2. Berlin: Springer-Verlag; 1973. p. 3-28.

Beckett EAH, McGeough CA, Sanders KM, Ward SM. Pacing of interstitial cells of Cajal in the murine gastric antrum: neural mediated and direct stimulation. J Physiol. 2003; 553:545–559. [PubMed: 14500772]

Berthoud H-R, Powley TL. Vagal afferent innervations of the rat fundic stomach: Morphological characterization of the gastric tension receptor. J Comp Neurol. 1992; 319:261–276. [PubMed: 1522247]

Bielefeldt K, Zhong F, Koerber HR, Davis BM. Phenotyping characterization of gastric sensory neurons in mice. Am J Physiol Gastrointest Liver Physiol. 2006; 291:G987–G997. [PubMed: 16728726]

Blackshaw LA, Grundy D, Scratcherd T. Vagal afferent discharge from gastric mechanoreceptors during contraction and relaxation of the ferret corpus. J auton Nerv Syst. 1987; 18:19–24. [PubMed: 3819312]

Brierley SM. Molecular basis of mechanosensitivity. Auton Neurosci: Basic and Clin. 2010; 153:58–68.

Brookes, SJH.; Zagorodnyuk, VP.; Costa, M. Mechanotransduction by vagal tension receptors in upper gut. In: Undem, BJ.; Weinreich, D., editors. Advances in Vagal Afferent Neurobiology. Boca Raton: CRC Taylor & Francis Group; 2005. p. 147-166.

Burns AJ, Lomax AEJ, Torihashi S, Sanders KM, Ward SM. Interstitial cells of Cajal mediate inhibitory neurotransmission in the stomach. Proc Natl Acad Sci. 1996; 93:12008–12013. [PubMed: 8876253]

Chang YZ, Hoover DB, Hancock JC. Endogenous tachykinins cause bradycardia by stimulating cholinergic neurons in the isolated pig heart. Am J Physiol. 2000; 278:R1483–R1489.

Cobine CA, Hennig GW, Bayguinov YR, Hatton WJ, Ward SM, Keef KD. Interstitial cells of Cajal in the cynomolgus monkey rectoanal region and their relationship to sympathetic and nitrergic nerves. Am J Physiol Gastrointest Liver Physiol. 2009; 298:G643–G656. [PubMed: 20150245]

Gabella, G. Structure of intestinal musculature. In: Schultz, SG.; Wood, JD.; Rauner, BB., editors. Handbook of Physiology, Section 6 The Gastrointestinal System. Vol. 1. American Physiological Society; 1989. p. 103-139.

Gokin AP, Jennings LJ, Mawe GM. Actions of calcitonin gene-related peptide in guinea pig gallbladder ganglia. Am J Physiol. 1996; 271:G876–G883. [PubMed: 8944703]

Goyal RJ, Chaudhury A. Mounting evidence against the role of ICC in neurotransmission to smooth muscle in the gut. Am J Physiol Gastrointest Liver Physiol. 2010; 298:G10–G13. [PubMed: 19892937]

Gulbins, J.; Glubins, R. Photographic multishot techniques: high dynamic range, super-resolution, extended depth of field, stitching. Rocky Nook; Santa Barbara, CA: 2009.

Huizinga JD, Reed DE, Berezin I, Wang X-Y, Valdez DT, Liu LWC, Diamant NE. Survival dependency of intramuscular ICC on vagal afferent nerves in the cat esophagus. Am J Physiol Regul Inegr Comp Physiol. 2008; 294:R302–R310.

Huizinga JD, Lammers WJEP, Mikkelsen HB, Zhu Y, Wang W-Y. Toward a concept of stretch coupling in smooth muscle: A thesis by Lars Thuneberg on contractile acitivity in neonatal interstitial cells of Cajal. Anat Rec. 2010; 293:1543–1552.

Iggo A. Is the physiology of cutaneous receptors determined by morphology? Prog Brain Res. 1976; 43:15–31. [PubMed: 1257472]

Jun JY, Choi S, Yeum CH, Chang IY, Park CK, Kim MY, Kong ID, So I, Kim KW, You HJ. Noradrenaline inhibits pacemaker currents through stimulation of beta(1)-adrenoceptors in cultured interstitial cells of Cajal from murine small intestine. British J Pharmacol. 2004; 141:670–677.

Kraichely RE, Farrugia G. Mechanosensitive ion channels in interstitial cells of Cajal and smooth muscle of the gastrointestinal tract. Neurogastroenterol Motil. 2007; 19:245–252. [PubMed: 17391240]

Lawrentjew BJ. Experimentel-morphologische Studien über den Aufbau des Ganglien des Spieserohre nebst einigen Bemerkungen über das Vorkommen und die Verteilung zweier Arten von Nervensellen im autonomen Nervensystem. Z Zellforsch Mikrosk Anat Forsch. 1929; 18:233–262.

Leek BF. Reticulo-ruminal mechanoreceptors in sheep. J Physiol. 1969; 202:585–609. [PubMed: 5789939]

Liem RSB, Willigen JD. UItrastructure of intra-epithelial nerve endings in the hard palate of the rat, Rattus Norvegicus. Archs Oral Biol. 1985; 30:461–466.

MacIver MB, Tanelian DI. Free nerve ending terminal morphology is fiber type specific for Aδ and C fibers innervating rabbit corneal epithelium. J of Neurophysiol. 1973; 69:1779–1783. [PubMed: 8509835]

Mitsui R, Komuro T. Direct and indirect innervation of smooth muscle cells of rat stomach, with special reference to the interstitial cells of Cajal. Cell Tissue Res. 2002; 309:219–227. [PubMed: 12172781]

Phillips RJ, Powley TL. Tension and stretch receptors in gastrointestinal smooth muscle: Reevaluating vagal mechanoreceptor electrophysiology. Br Res Rev. 2000; 34:1–26.

Powley TL, Phillips RJ. Musings on the wanderer: What's new in our understanding of vago-vagal reflexes? I. Morphology and topography of vagal afferents innervating the GI tract. Am J Physiol Gastrointestinal Liver Physiol. 2002; 283:G1217–1225.

Powley, TL.; Phillips, RJ. Advances in neural tracing of vagal afferent nerves and terminals. In: Undem, BJ.; Weinreich, D., editors. Advances in Vagal Afferent Neurobiology. CRC Press; Boca Raton: 2005.

Powley TL, Wang X-Y, Fox EA, Phillips RJ, Liu LWC, Huizinga JD. Ultrastructural evidence for communication between intramuscular vagal mechanoreceptors and interstitial cells of Cajal in the rat fundus. Neurogastroenterol Mot. 2008; 20:69–79.

Raab M, Neuhuber WL. Intraganglionic laminar endings and their relationships with neuronal and glial structures of myenteric ganglia in the esophagus of rat and mouse. Histochem and Cell Biol. 2004; 122:445–459. [PubMed: 15378379]

Rodrigo J, Hernández J, Vidal MA, Pedrosa JA. Vegetative innervation of the esophagus. II. Intraganglionic laminar endings. Acta Anat. 1975; 92:79–100. [PubMed: 1163197]

Salmhofer H, Neuhuber WL, Ruth P, Huber A, Russwurm M, Allescher HD. Pivotal role of the interstitial cells of Cajal in the nitric oxide signaling pathways of rat small intestine – Morphological evidence. Cell and Tissue Res. 2001; 305:331–340. [PubMed: 11572086]

Sanders, KM.; Koh, SD. Stretch-activated conductances in smooth muscles. In: Hamill, OP., editor. Mechanosensitive Ion Channels, Part B, Current Topics in Membranes. Vol. 59. Amsterdam: Academic Press, Elsevier; 2007. p. 511-540.

Sanders KM, Hwang SJ, Ward SM. Neuroeffector apparatus in gastrointestinal smooth muscle organs. J Physiol. 2010; 588:4621–4639. [PubMed: 20921202]

Smid, SD. Neuronal mechanosensitivity in the gastrointestinal tract In: Mechanosensitivity of the Nervous System. In: Kamkin, A.; Kiseleva, I., editors. Mechanosensitivity in Cells and Tissues. Vol. 2. Springer; 2009. p. 87-103.

Wang FB, Powley TL. Topographic inventories of vagal afferents in gastrointestinal muscle. J Comp Neurol. 2000; 421:302–324. [PubMed: 10813789]

Ward SM, Beckett EAH, Wang XY, Baker F, Khoyi F, Sanders KM. Interstitial cells of Cajal mediate cholinergic neurotransmission from enteric motor neurons. J Neurosci. 2000; 20:1393–1403. [PubMed: 10662830]

Ward SM, Sanders KM. Interstitial cells of Cajal: Primary targets of enteric motor innervation. Anat Rec. 2001; 262:125–133. [PubMed: 11146435]

Wei JY, Adelson DW, Taché Y, Go VLW. Centrifugal gastric vagal afferent unit activities: another source of gastric "efferent" control. J auton Nerv Syst. 1995; 52:83–97. [PubMed: 7615902]

Won K-J, Sanders KM, Ward SM. Interstitial cells of Cajal mediate mechanosensitive responses in the stomach. PNAS. 2005; 102:14913–14918. [PubMed: 16204383]

Zagorodnyuk VP, Chen BN, Brookes SJH. Intraganglionic laminar endings are mechano-transduction sites of vagal tension receptors in the guinea-pig stomach. J Physiol. 2001; 534:255–268. [PubMed: 11433006]

Zagorodnyuk VP, Brookes SJH, Spencer NJ. Structure-function relationships of sensory endings in the gut and bladder. Auton Neuro Sci: Basic and Clinical. 2010; 153:3–11.

Zhang Y, Carmichael SA, Wang X-Y, Huizinga JD, Paterson WG. Neurotransmission in lower esophageal sphincter of W/W^{v} mutant mice. Am J Physiol Gastrointest Liver Physiol. 2010; 298:G14–G24. [PubMed: 19850967]

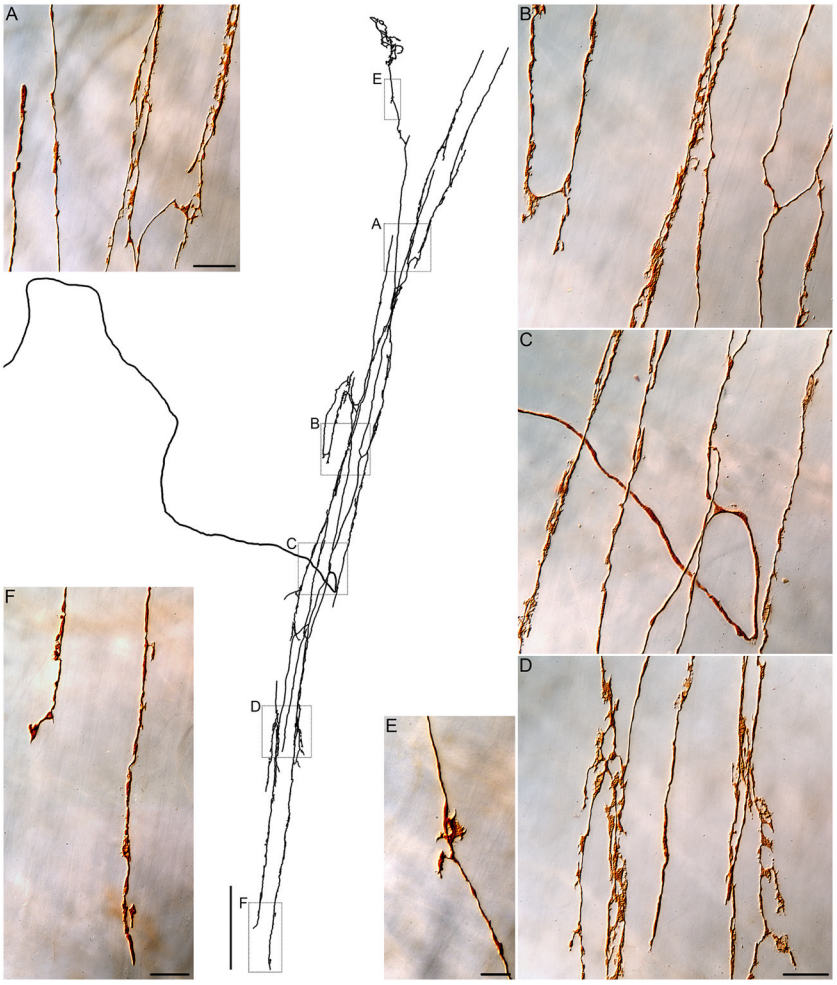

Figure 1.

A vagal intramuscular array or IMA. In the center of the figure, a tracing of a complete terminal arbor in circular muscle of the corpus is presented in monochrome. The parent neurite enters from the left, courses to the terminal field, loops, and then arborizes repeatedly to produce the afferent array. Panels A through F are photomicrographs of the afferent that was traced (taken at the locations delineated by boxes on the tracing) illustrating the finer details of the terminal array of the IMA. To highlight the structure of the arbor, this specimen was prepared by processing the whole mount for the dextran label, but omitting any double-labeling. In Panel C, Photoshop was used to remove a distracting piece of DAB artifact. Scale bars: Tracing panel: 250 μm; Panel A: 20 μm; Panel D: 20 μm, applies to B, C and D; Panel E: 10 μm; Panel F: 20 μm.

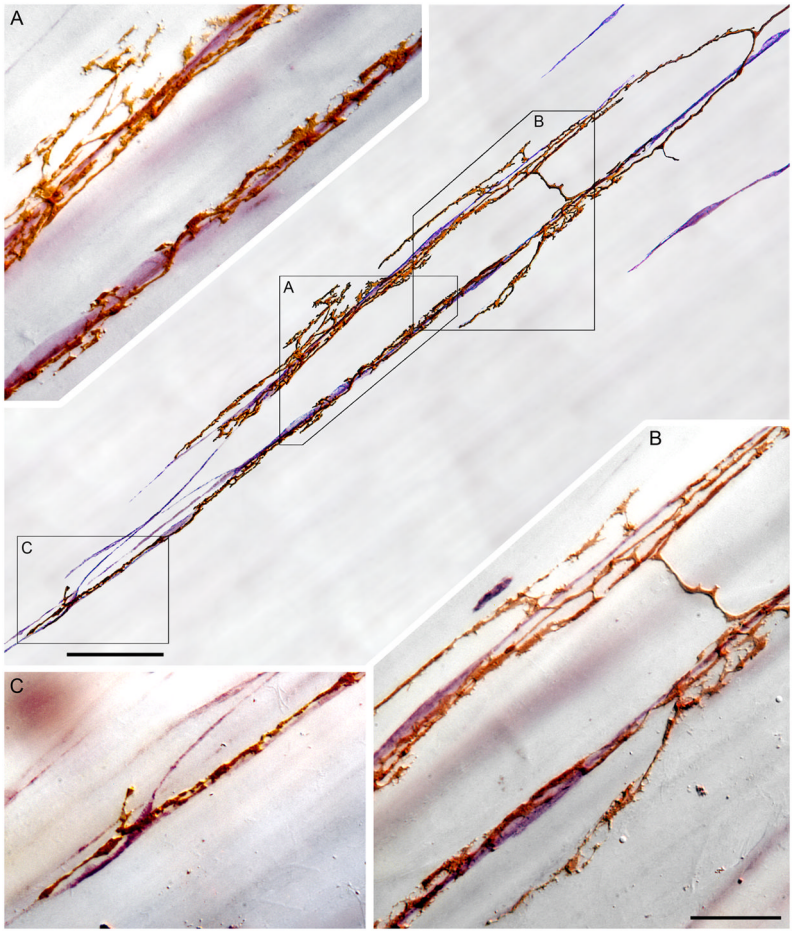

Figure 2.

A segment of an intramuscular array-interstitial cell of Cajal (IMA-ICC) complex. In the central panel of the figure, a tracing illustrates two collateral neurites of an IMA (golden brown, DAB processing) coursing along and forming varicosities and lamellar contacts on two adjacent strings of ICCs (violet; Vector VIP processing for cKit). Panels A through C are photomicrographs (taken at the locations designated by boxes on the tracing) that illustrate the pattern of the IMA-ICC appositions. Panels A and B also illustrate short parallel side arms or spurs of the neurites that extend off the chains of ICCs and into bands of (unstained) smooth muscle fibers. Panel B also illustrates a characteristic bridging element spanning between the neurite processes innervating the two strings of ICCs. Scale bars: Tracing panel: 50 μm; Panel B: 20 μm, applies to panels A, B, and C.

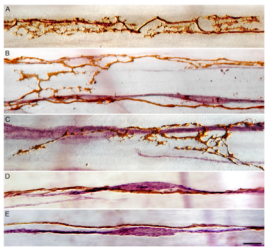

Figure 3.
High power (100X objective) illustrations of the variety of varicose and lamellar appositions formed by IMAs on ICCs. The complexity of apparent appositions between IMAs and ICCs ranges from elaborate and lamellar varicosities (Panels A, B and C) to subtle dilations or swellings of relatively smooth neurites coursing along the ICCs (Panels D and E). Panel A: a labeled IMA is shown without ICC counterstaining in order to accentuate the complexity of lamellar varicosities observed. Panels B, C, D and E illustrate the range of complexity of tracer-labeled IMA appositions (DAB processing, brown) seen in conjunction with ICCs (cKit immunohistochemistry with Vector VIP, violet). Scale bar in Panel E, for all panels: 10 μm.

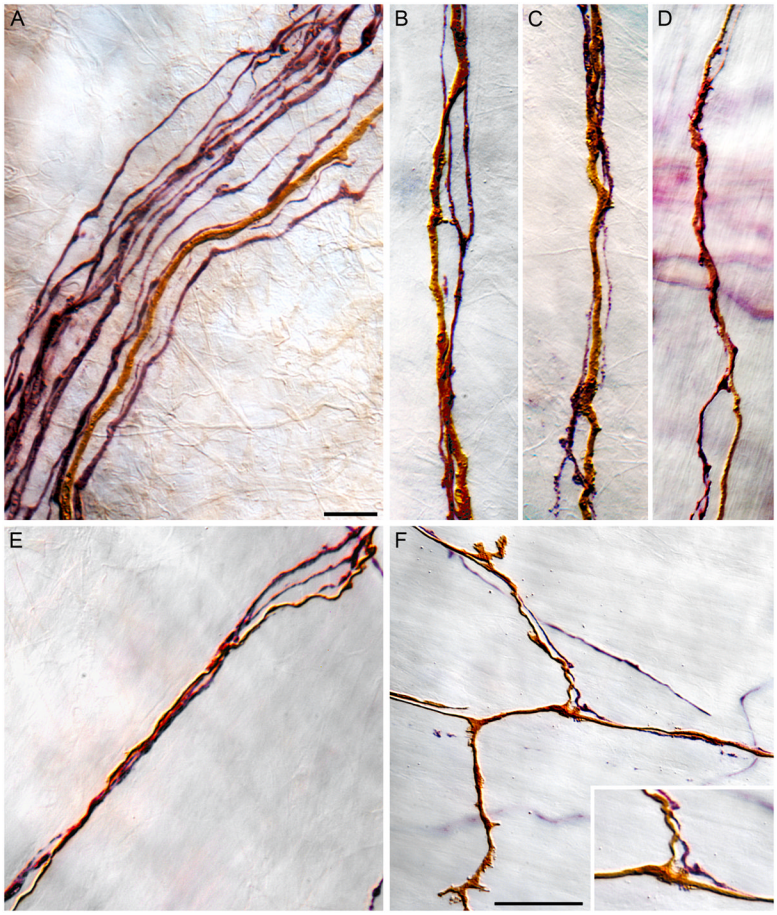

Figure 4.

CGRP-positive fibers coursing with dextran-labeled IMA afferent fibers to innervate IMA-ICC complexes. Panel A illustrates a bundle of fibers traveling in the stomach wall proximal to the final bifurcations into terminal fields. One dextran-labeled IMA fiber (DAB, brown) courses in conjunction with several presumptive visceral afferents expressing CGRP (immunostained with Vector VIP, violet). Panels B through E illustrate “final” fascicles of fibers in close proximity to an IMA terminal. As illustrated, individual vagal IMA afferents (DAB, brown) course in the fine fascicles with one or two CGRP-positive (presumably) visceral afferent fibers. In some instances, IMA afferent and CGRP-positive neurites contain swellings that would be consistent with axo-axonic interactions. Panel F illustrates a region of an IMA (DAB labeling, brown), including segments of the neurites that parallel the muscle fibers (horizontal axis in this photomicrograph) and bridging elements (vertical axis), that contains an intermingling CGRP-positive neurite (Vector VIP, violet). Panel F inset is a higher power view of the bifurcation that occurs in the middle of panel F. The IMA neurite and the CGRP+ neurite appear to have varicosities in close apposition to each other. Scale bars: Panel A: 10 μm, applies to panels A, B, C, D, E, and the insert in panel F. Panel F: 25 μm.

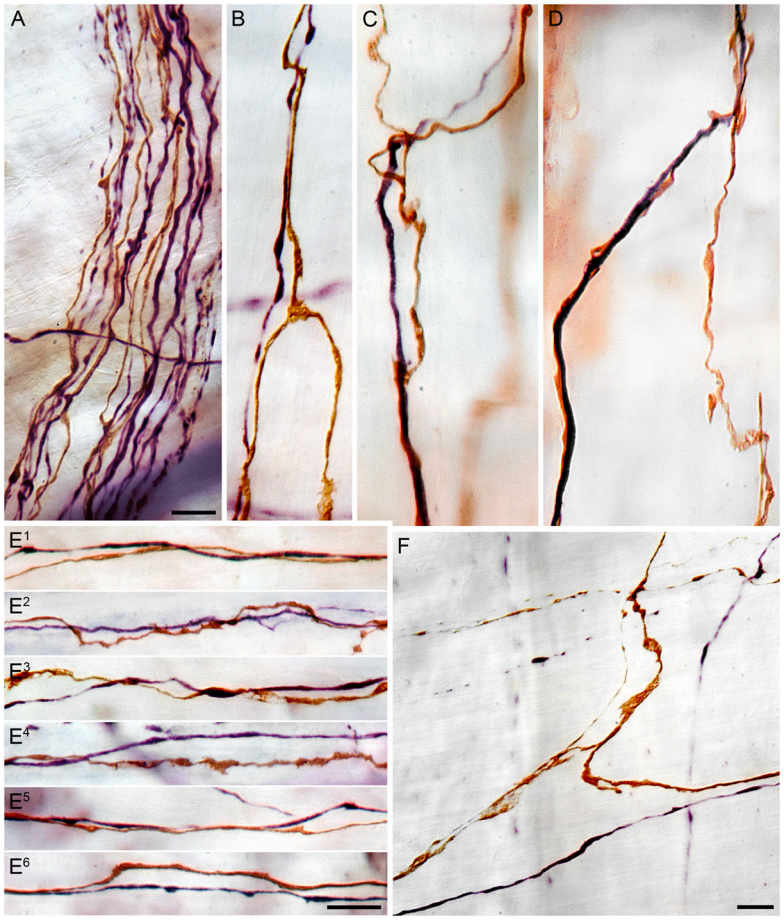

Figure 5.
Catecholaminergic or tyrosine hydroxylase-positive fibers course in conjunction with vagal IMA neurites as they travel through bundles and fascicles in the gastric wall and as they form the terminal arrays of the IMAs. Panel A illustrates a bundle of fibers located proximally in the wall of the stomach that contains several IMA fibers (DAB, brown) and several TH+ axons (Vector VIP, violet). Panels B, C, D and F illustrate single TH+ (Vector VIP, violet) axons co-mingling with the parallel neurites and bridging fibers of individual IMAs. Panels E^1 through E^6 illustrate individual TH+ fibers (Vector VIP, violet) running in tandem with long parallel neurites of IMAs (DAB, brown) within the arrays. Both the (presumptively sympathetic efferent) TH+ fibers and the vagal afferent IMA fibers contain varicosities that could be *en passage* appositions. Scale bars: Panel A: 10 μm; Panel D: 10 μm, applies to panels B, C, and D; Panel E^6: 10 μm, applies to panels E^1 through E^6; Panel F: 10 μm.

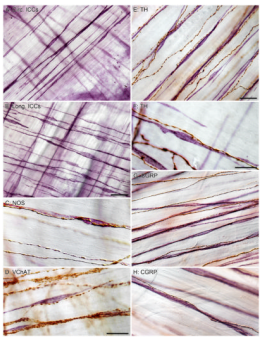

Figure 6.

ICCs of the intramuscular type, the type that forms complexes with IMAs, also are innervated by other afferent (e.g., CGRP+) as well as efferent (TH+, NOS+, and VChAT+) fibers. Panels A and B illustrate the parallel strings of ICCs (Vector VIP stained) found in both circular (panel A) and longitudinal (panel B) that appear to serve as accessory tissue scaffolding for vagal IMAs. Panel C illustrates, as previously described (e.g., Salmhofer et al., 2001), NOS+ fibers (DAB, brown) are observed in tight association with ICCs (Vector VIP, violet); Panel D depicts, as has been previously reported (e.g., Ward et al., 2000), that cholinergic or VChAT+ fibers (DAB, brown) also appear to course so as to make contact with chains of ICCs (Vector VIP, violet); Panels E and F illustrate that catecholaminergic or TH+ axons (DAB, brown), as has been reported (e.g., Cobine et al., 2009), course in tight registration with the ICC scaffolds; Panels G and H illustrate the fact that (presumably visceral afferent) CGRP+ axons (DAB, brown) also course on or in conjunction with the chains of ICCs (Vector VIP, violet) with which vagal IMAs form complexes. Scale bars: Panel A: 40 μm, applies to panels A and B; Panel C: 20 μm, applies to panels C and D; Panel E: 25 μm, applies to panels E and G; Panel F: 20 μm, applies to panels F and H.

Table 1

List of primary and secondary antisera

	Dilution	Supplier (code)
Primary		
Mouse Calcitonin gene-related peptide (CGRP)	1:10,000	CURE/Digestive Disease Research Center (4901)
Goat c-Kit (M-14) Tyrosine Kinase Receptor	1:1,000	Santa Cruz Biotech., Santa Cruz, CA (sc-1494)
Rabbit Nitric oxide synthase (NOS)	1:500	AbD Serotec, Raleigh, NC (AHP477)
Mouse Tyrosine hydroxylase (TH)	1:1,000	ImmunoStar Inc., Hudson, WI (22941)
Rabbit Vesicular acetylcholine transporter (VAChT)	1:1,500	Sigma-Aldrich, St Louis, MO (V5387)
Secondary		
Donkey Biotin-SP Goat	1:500	Jackson Immuno., West Grove, PA (705-065-147)
Donkey Biotin-SP Rabbit	1:500	Jackson Immuno., West Grove, PA (711-065-152)
Horse Biotinylated Goat	1:1,000	Vector Laboratories, Burlingame, CA (BA-9500)
Horse Biotinylated Mouse	1:200	Vector Laboratories, Burlingame, CA (BA-2001)